PROBE MEASUREMENTS IN THE ASDEX BOUNDARY LAYER AND THE EFFECT OF NEUTRAL BEAM INJECTION AND LOWER HYBRID HEATING

M. El Shaer[+]

IPP III/96

April 1984

MAX-PLANCK-INSTITUT FÜR PLASMAPHYSIK

8046 GARCHING BEI MÜNCHEN

MAX-PLANCK-INSTITUT FÜR PLASMAPHYSIK

GARCHING BEI MÜNCHEN

PROBE MEASUREMENTS IN THE ASDEX BOUNDARY LAYER AND THE EFFECT OF NEUTRAL BEAM INJECTION AND LOWER HYBRID HEATING

M. El Shaer[+]

IPP III/96 April 1984

[+]permanent address: Faculty of Engineering, EL ZAGAZIG University, EL ZAGAZIG, EGYPT

Die nachstehende Arbeit wurde im Rahmen des Vertrages zwischen dem Max-Planck-Institut für Plasmaphysik und der Europäischen Atomgemeinschaft über die Zusammenarbeit auf dem Gebiete der Plasmaphysik durchgeführt.

IPP III/96 M. El Shaer[+] PROBE MEASUREMENTS IN THE ASDEX BOUNDARY LAYER AND THE EFFECT OF NEUTRAL BEAM INJECTION AND LOWER HYBRID HEATING

ABSTRACT

The electron temperature and density in the ASDEX main chamber boundary plasma are measured using a movable double probe. From the measured density and temperature profiles we can deduce characteristic decay lengths illustrating the transport in this particular region out of the separatrix. The effects of two types of heating are investigated, during the neutral beam injection the boundary plasma seems to respond to the high and low ß regimes found in ASDEX. The lower hybrid heating affects the boundary plasma by increasing the electron temperature and modifying the density profile.

[+] permanent address: Faculty of Engineering, EL ZAGAZIG University, EL ZAGAZIG, EGYPT

Probe measurements in the ASDEX boundary layer and the effect of neutral beam injection and lower hybrid heating

M. El Shaer

1. Introduction

The parameters of the boundary-layer in tokamaks with limiter or divertor configurations are still very interesting for studying plasma transport and the effect of various types of heating.

Measurements of the boundary plasma parameters in divertor configurations can also help towards understanding the mechanisms of particle and energy flow to the wall and to the divertor chamber.

The measurements described here were made in the ASDEX main plasma boundary layer with a movable double probe, in order to determine the decaying characteristic length of the density and temperature profiles up to the wall and to show the effect of neutral beam injection (NBI) and lower hybrid (LH) heating on the parameters of the ASDEX boundary layer.

2. Description of the probe and measuring method

The measuring range extends from the separatrix to the wall radius. In this region the use of Langmuir probes is the simplest way to measure the density and electron temperature.

The probe used is shown in Fig. 1. The tips of the probe are made of molybdenum, 1 mm in diameter and 2 mm long, and are perpendicular to the main magnetic field, the one probe tip casting no shadow on the other.

The probe is moved with a manipulator, and the two probe tips can easily be replaced.

The electric circuit used is shown in Fig. 2. A sawtooth delivered by a function generator is amplified by a Kepco amplifier and applied to the probe. The current is measured across a resistance and the voltage across a divider. The current and voltage are applied to the data acquisition system via two isolated amplifiers.

The voltage applied is in the range of ±75 V and the current collected does not exceed 50 mA.

Figure 3 shows an example of the collected current for an applied sawtooth voltage.

A detailed treatment of the particle collections by the probe is described in Ref. /1/. The electron temperaure is given by

$$T_e = \frac{I_{sat}}{2\ [\frac{dI}{dV}]_o} \quad \text{(in eV)},$$

where I_{sat} is the probe ion saturation current, and $[\frac{dI}{dV}]_o$ is the slope of the I-V characteristic passing through zero. The ion saturation current can be written in a simple form, secondary effects being neglected, as follows:

$$I_{sat} = 0.6\, en_e\, S\, [k(\frac{T_e+T_i}{m_i})]^{1/2},$$

where T_i is the ion temperature, and S the probe surface, taken as twice the probe cross-sectional area perpendicular to the magnetic field.

If $T_i = T_e$, this an be written as

$$n(cm^{-3}) = \frac{0.75\ 10^{12}\ I_{sat}(mA)\ \sqrt{M_A}}{S(mm^2)\ \sqrt{T_e\ (eV)}},$$

where M_A is the gas atomic mass.

The probe is a simple diagnostic, but the measuring method is subject to many limitations and uncertainties. The main difficulty in measuring with probes in the boundary layer of a tokamak with divertor configuration is the absence of protection for the probe when the plasma moves to the wall after a disruption, which may lead to destruction of the probe.

The probe is also exposed to relatively high density. The elevation of the temperature of the probe Tip measured with a thermocouple 5 cm from the separatrix (which has a radius of 40 cm) is shown in Fig. 4. The temperature rise of the Tip is 400°C in normal operation. Fortunately, the probe is easily cooled by conduction during the time intervals between shots. The probe is always kept a few cm from the separatrix in order to limit the heat flux to

the probe from the plasma.

3. Typical characteristics of the ASDEX boundary layer

ASDEX is a double-null divertor tokamak with a major radius of 165 cm and a nominal minor radius of 40 cm, a toroidal magnetic field $B_T \leq 2.8$ TD and a plasma current $I_p \leq 500$ kA /2/.

As in limiter discharge configurations, the plasma boundary in the divertor configuration is formed by diffusion of the main plasma toward the wall.

Figure 5 shows two radial profiles of the boundary density (n_b) for two main average densities. The density measurements extend from a few cm inside the separatrix radius, which is at 38 cm in this case, toward the wall. The inner part of the profile is measured by Thomson scattering /3/, giving a 1/e characteristic decay length λ_n of about 2.3 cm, while further out the measured values are obtained with the probe. Within the error bars, in the overlap region the values given by the two methods are in agreement.

The profile obtained with the probe is flatter with λ_n = 4.5 cm, but around a radius of 45 cm the profile again becomes steeper with λ_n = 2.5 cm. In Fig. 6 the electron temperature (T_b) profiles are also shown, the characteristic decay length λ_T being 7 cm.

It is seen in Fig. 5 that after the separatrix we have two distinct regions characterized by the change in λ_n, this change occurring approximately between 44 and 45 cm, which is the radius where the field lines extending from the main chamber to the divertor chamber impinge on the protective plates of the divertor coils, causing the shortness of the particle trajectory in the direction of the divertor.

If one takes $\lambda_n = \sqrt{\tau_{\parallel} D_{\perp}}$, where $\tau_{\parallel}$ is the particle diffusion time along the field line to the divertor and $D_{\perp}$ ist the diffusion coefficient perpendicular to the toroidal field lines, then the reduction of λ_n may be caused by the reduction in $\tau_{\parallel}$, which is a consequence of the shortness of the particle trajectory to the divertor, if $D_{\perp}$ is assumed to be unchanged.

The recuction in λ_n proves that the equilibrium in the boundary layer is a composite of two motions, one perpendicular to the main toroidal magnetic

field and the other along the field line to the divertor.

The relation between the main plasma and the boundary plasma is shown in Fig. 7, where n_b is given for a radius of 41 cm. The boundary density is exponentially proportional to the main average density and the boundary electron temperature is inversely proportional to it.

In Fig. 8 the effect of inserting a mushroom-type limiter on the boundary parameters is shown. The density profile seems to flatten and the temperature profile becomes steeper, this result possibly being due to the particular geometry of the field lines induced by this type of limiter.

4. Effect of applying neutral beam heating on the boundary layer parameters

The neutral beam injection (NBI) induced an increase in the probe ion saturation current on application of the beam.

Figure 9 shows the similarity between the H_α signal measured with a photodiode in the divertor chamber and the signal obtained with the probe biased with a constant voltage. The probe signal is smoothed with an appropriate smoothing factor to eliminate the noise. This indicates that the plasma in the boundary layer and in the divertor are closely related. From Fig. 10 one can also identify the two regimes found in ASDEX during NBI with a divertor configuration /4/: The high-ß (H) and low-ß (L) regimes.

After the purely ohmic phase (OH), NBI first induces an increase in the ion saturation current during the L phase, followed by a decrease corresponding to the H phase, which leads to the occurrence of bursts announcing the deterioration of the H regime.

The ion saturation current collected by the probe is plotted in Fig 10 versus the radius for the three regimes, the value taken as the H regime being the value without bursts.

The density and the electron temperature in the three regimes are plotted in Fig. 11, the density in the L regime being approximately twice as high as in the OH regime. The radial profile of the H regime is much steeper with $\lambda_n = 3$ cm than the OH or L regime with $\lambda_n = 4.5$ cm. This may be explained as a consequence of the good confinement, which lowers the diffusion coefficient.

(The absolute value of the density in Fig. 12 is excessively high owing to the bad condition of the probe for these shots.) The electron temperatures in the three regimes are not very different from one another. We can, however, note a small increase during the H regime.

Figure 12 shows the relative increase in the burst amplitude, I_{burst} compared with the steady saturation current I_{sat}, in the H regime without bursts. The increase of this ratio in the outer region is due to two competing effects, the increase in the burst amplitude and the decrease in the ion saturation current as shown in Fig. 10. However, in a region close to the wall the rapid increase in the ratio $\frac{I_{burst}}{I_{sat}}$ is more sensitive to the increase in the burst amplitude than to the decrease in the ion saturation current.

5. Lower hybrid heating effects on the boundary layer parameters

As in the case of NBI, the boundary layer plasma responds to the high-frequency heating (HF) at the lower hybrid frequency (LH).
The effect of the HF is investigated with a double probe situated approximately 1 m toroidally apart from the HF coupler.

In ASDEX the wave is launched with an 8-waveguide grill /5/ at a frequency of 1.3 GHz. During these measurements the incident power was in the range of 500 kW and the grill position was 48 cm.

The application of the HF induces a change in density as shown in Fig. 13. The HF creates a depression in the density facing the grill and an increase behind it. It can also be seen in Fig. 13 for the OH phase, that a change of slope occurs in the density profile at the grill radius. This may be due to the interception of the flux line by the grill, which plays the role of a limiter and changes the equilibrium of the flowing particles to the wall and divertor chamber.

The electron temperature profile is also modified (Fig. 14). The relative increase of T_e is larger near the wall than near the grill mouth, at which the temperaure increases from 3 eV to 7 eV.

The density gradient is found to be 2.5×10^{11} cm^{-4} for an absolute density facing the grill of about 2×10^{11} cm^{-3}. The computation of these values with the measured reflection coefficients agrees with a coupling theory taking into

account the real density facing the grill and a reasonable density gradient /6/.

The modifications in density and temperature profiles have already been observed in WEGA /7/. Such phenomena are still open to many interpretations.

We can here interpret the depression occurring in the density profile in Fig. 15 as being a result of the increase in oscillated energy of the electrons in the region facing the grill, where the HF field is strong.

For this series of measurements the absorbed input power was negligibly, and so if we consider the plasma pressure along a toroidal flux line to be constant, then the increase in the electron energy should be accompanied by a decrease in density.

The increase in density behind the grill can be explained as a result of the ionization of the neutral gas when the electron temperature increases from 2 - 3 eV to 6 - 7 eV.

The probe measurements in the presence of the HF field can be subject to many ucertainties. This can be avoided, however, if the ions are not perturbed by the HF field owing to their weight compared with that of the electrons, and if the main change takes the form of an increase or decrease in the ion saturation current of the probe.

Only the electrons are accelerated in the HF field and may gain sufficient energy to alter the equilibrium in the region facing the grill. The probe was not affected by changes in the potential of the plasma during the HF, because as a double probe it follows any change in this potential.
The effect of secondary electron emission is not very important either in changing the value of the probe current. This effect needs a large value of density and temperature, which is not the case even during the application of the HF.

6. Conclusion

The parameters of the boundary layer are influenced by the existence of the divertor. The diffusion in the boundary layer is a composite of two motions, one perpendicular to the toroidal field and the other parallel to the field

lines to the divertor chamber.

The boundary layer is an important field of study as regards external types of heating.
During neutral beam injection, we can follow the two regimes of high and low ß found in ASDEX in the parameters of the boundary layer. The L regime is characterized by an icnreasse in density, and the H regime by a steepness in the denstiy profile. During the H regime, the relative increase in the burst amplitude is maximum near the wall.

Heating at the lower hybrid frequency affects the boundary layer by changing the density and temperature profiles. The density decreases facing the grill and increases behind it. The electron temperature is also increased everywhere. This effect can be explained by the fact that, owing to the electron temperature increase, the density decreases facing the grill to keep the pressure constant along a field line and increases near the wall as a result of neutral gas ionization.

Acknowledgements

The author wishes to thank the ASDEX-Team, especially Dr. Keilhacker, for fruitful discussions and help. The contributions of the LH-Team and the CEN-Grenoble-Team were essential for this work.

References

/1/ F.F. Chen, Plasma Diagnostics Techniques, Huddlestone and Leonard, Academic Press; P.C. Stangeby, J. Phys. D15, 1007 (1982).

/2/ M. Keilhacker, et al., "Impurity Control Experiments in the ASDEX Divertor", Proc. 8th Int. Conf. on Plasma Physics and Contr. Fusion Research, Brussels 1980, Vol. II, IAEA, Vienna (1981) 351.

/3/ H. Murmann, private communication.

/4/ M. Keilhacker, et al., "Confinement Studies in L and H Type ASDEX Discharges", Plasma Physics and Controlled Fusion, Vol. 26, No. 1A, pp 49-63, 1984.

/5/ H. Brinkschulte, et al., "The Lower Hybrid Heating Programme for ASDEX" 2nd Grenoble-Varenna Int. Symposium on Heating in Toroial Plasmas, Como, Sept. 1980.

/6/ M. Brambila and F. Leuterer, private communication.

/7/ M. El Shaer, G. Ichtchenko, "Experimental Measurements and Modelling of the WEGA Boundary Layer Plasma", EUR-CEA.FC 1197, 1983.

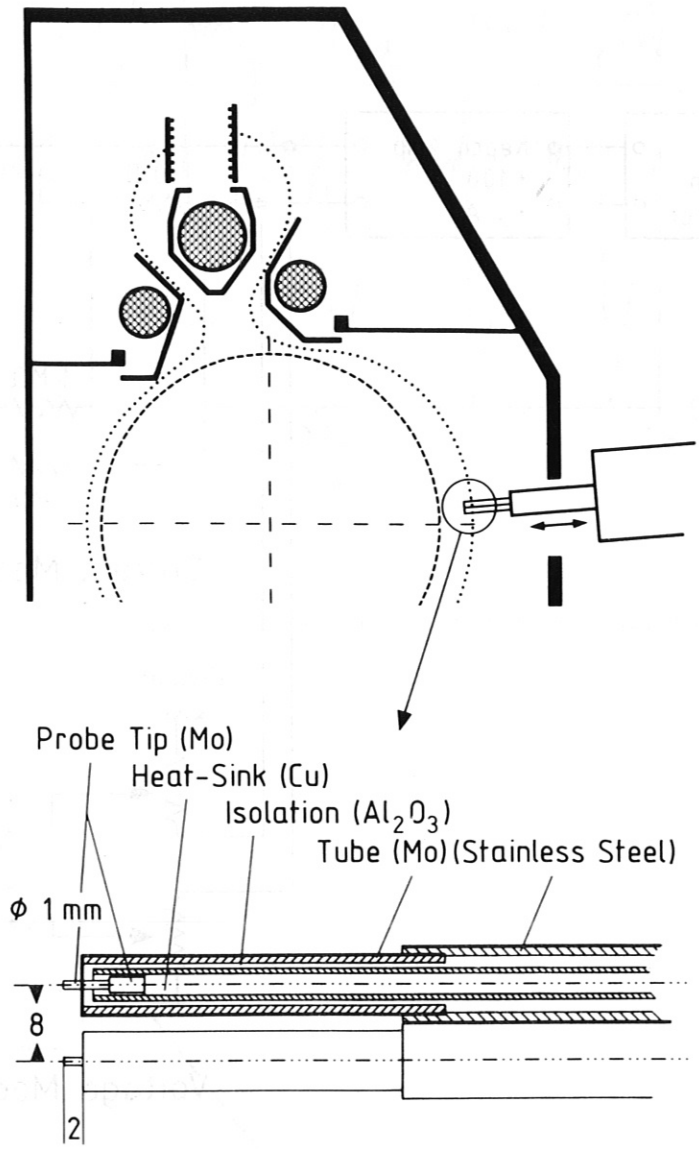

Fig. 1:
ASDEX cross-section showing the probe location, and a section of the probe.

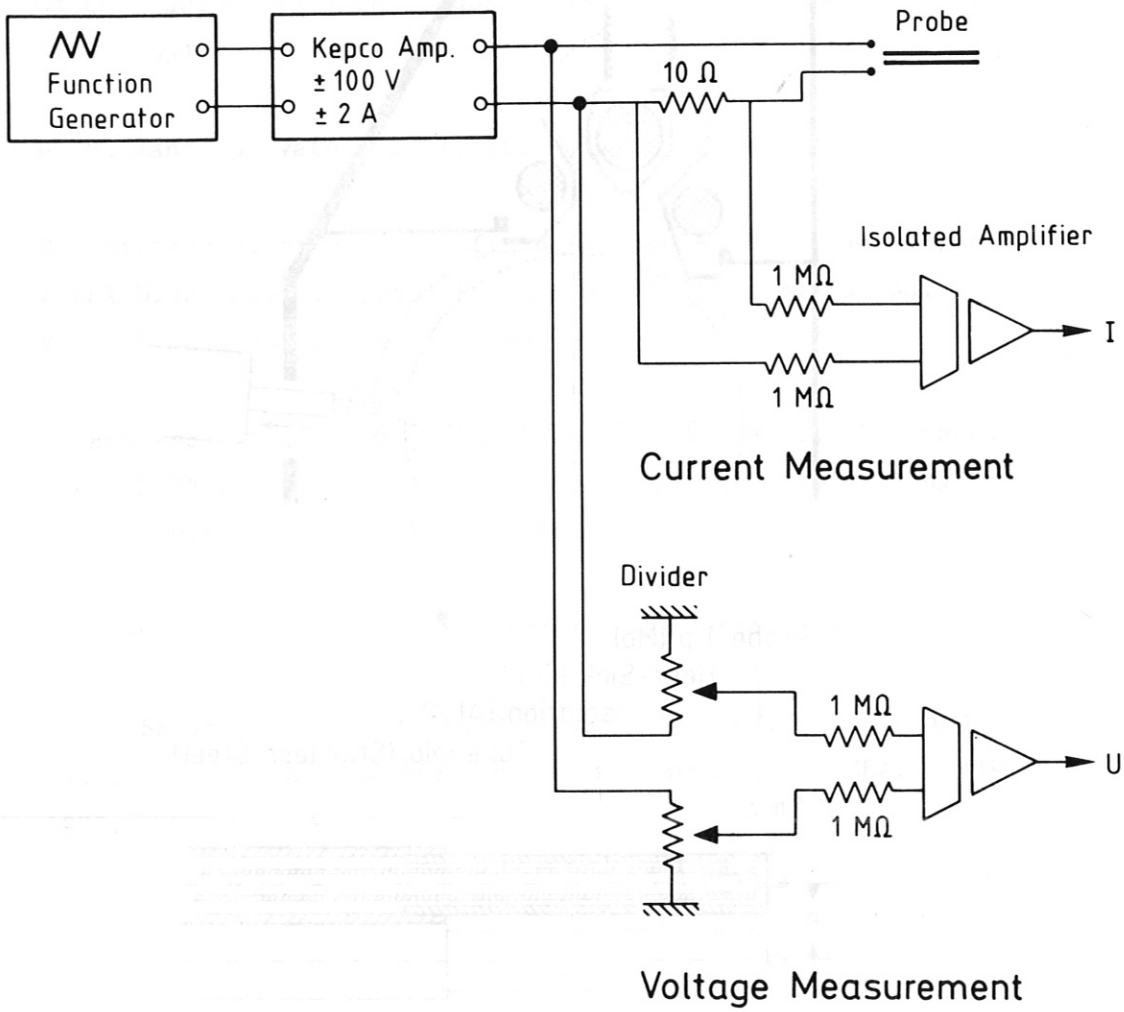

Fig. 2:
Probe electric circuit for voltage application and current collection.

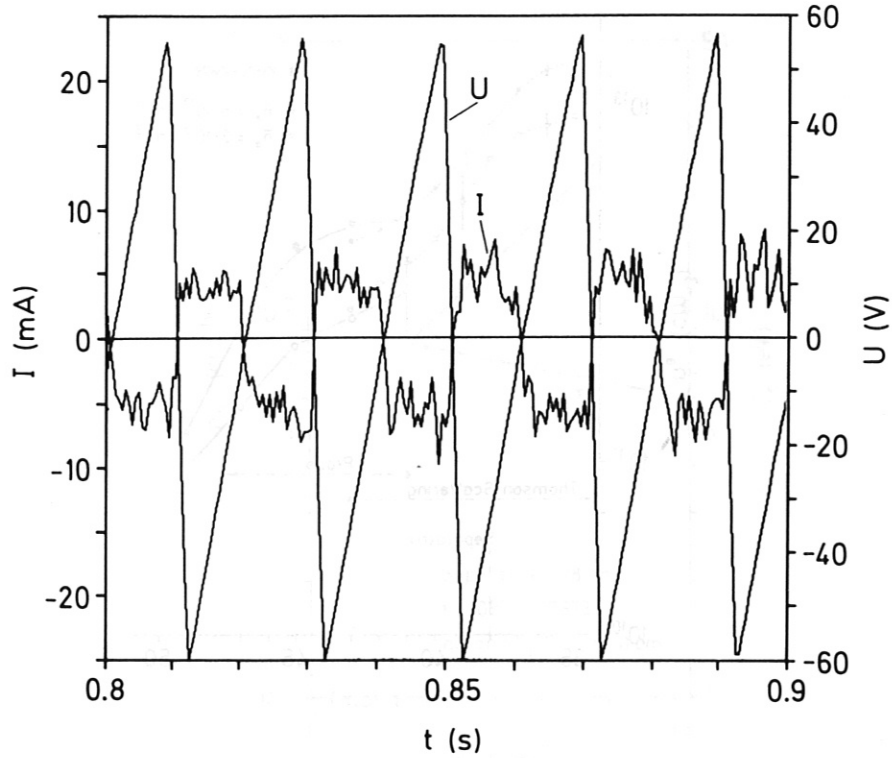

Fig. 3:
Probe characteristics showing the probe ion saturation current corresponding to the sawtooth voltage.

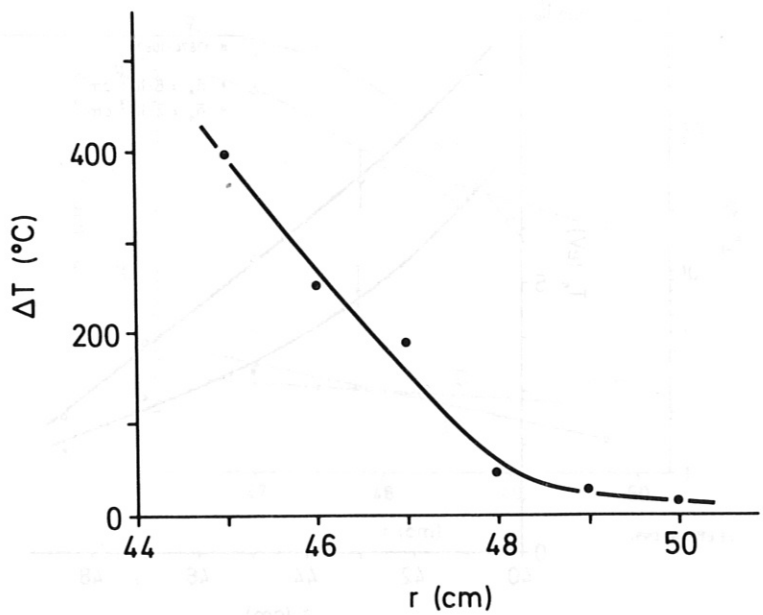

Fig. 4:
Relative increase of the temperature of the probe tip measured with a thermocouple.

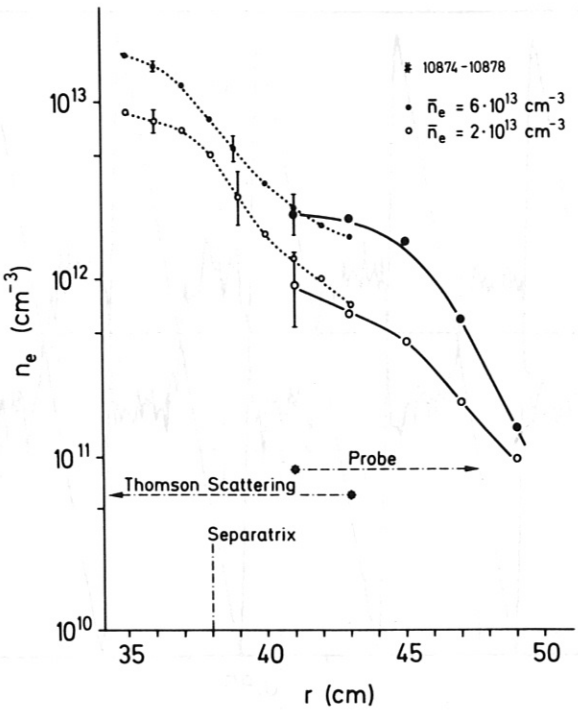

Fig. 5:
Radial profiles of the boundary density for 2 main average densities 2 x 10^{13} and 6 x 10^{13} cm^{-3}; the inner part is measured by Thomson scattering.

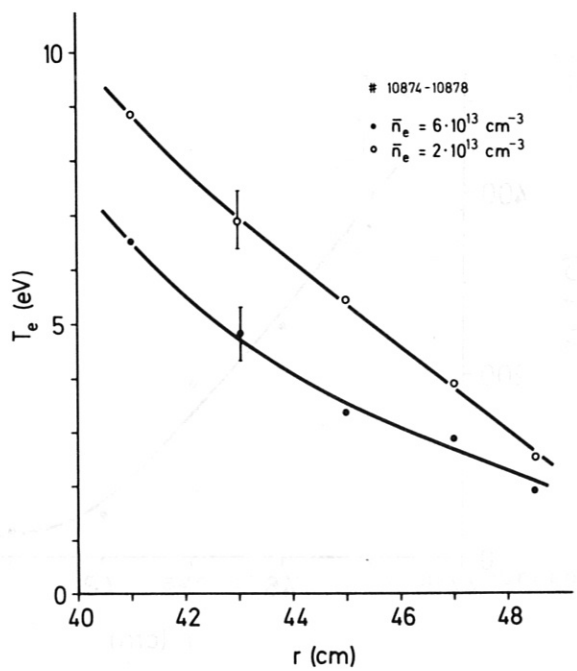

Fig. 6:
Electron temperature corresponding to the profiles of Fig. 5.

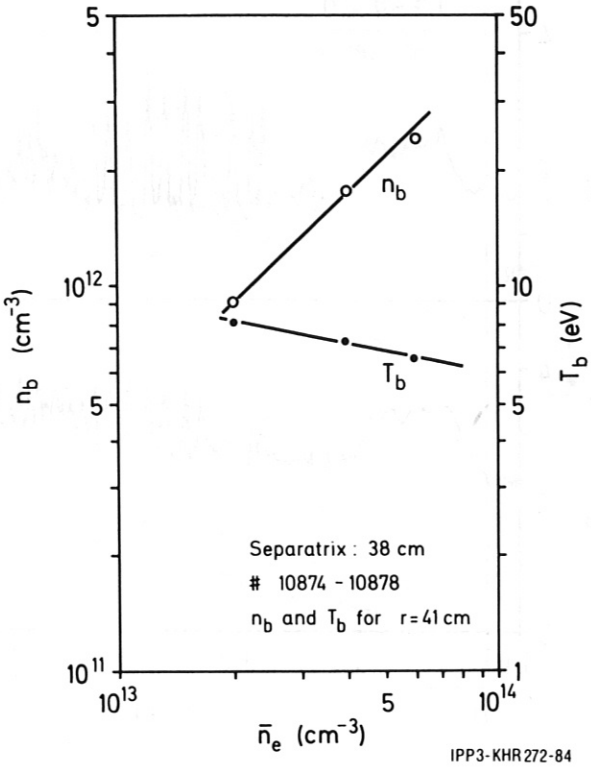

Fig. 7:
Relation between the boundary density and the average mean density; the boundary density is recorded at 41 cm.

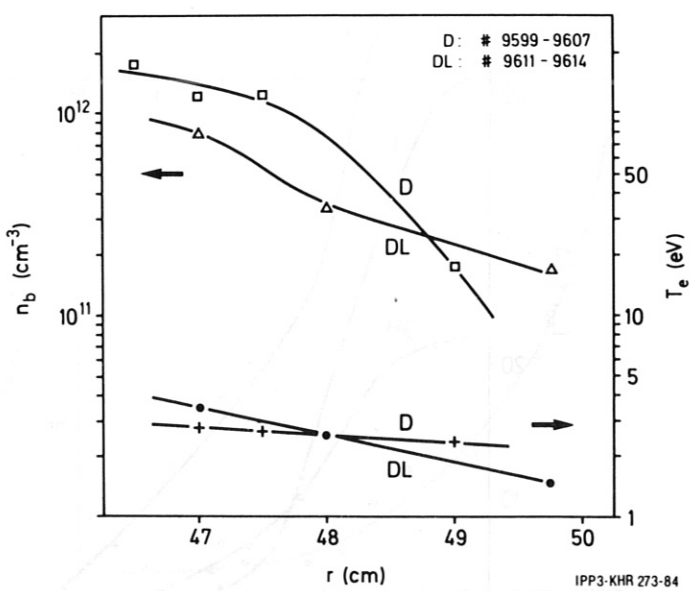

Fig. 8:
Comparison between the boundary density and temperature profiles of a divertor discharge (D) and divertor with a mushroom limiter configuration (DL); the position of the limiter was 42 cm (except for the last point at 50 cm, for which the limiter position was 45 cm).

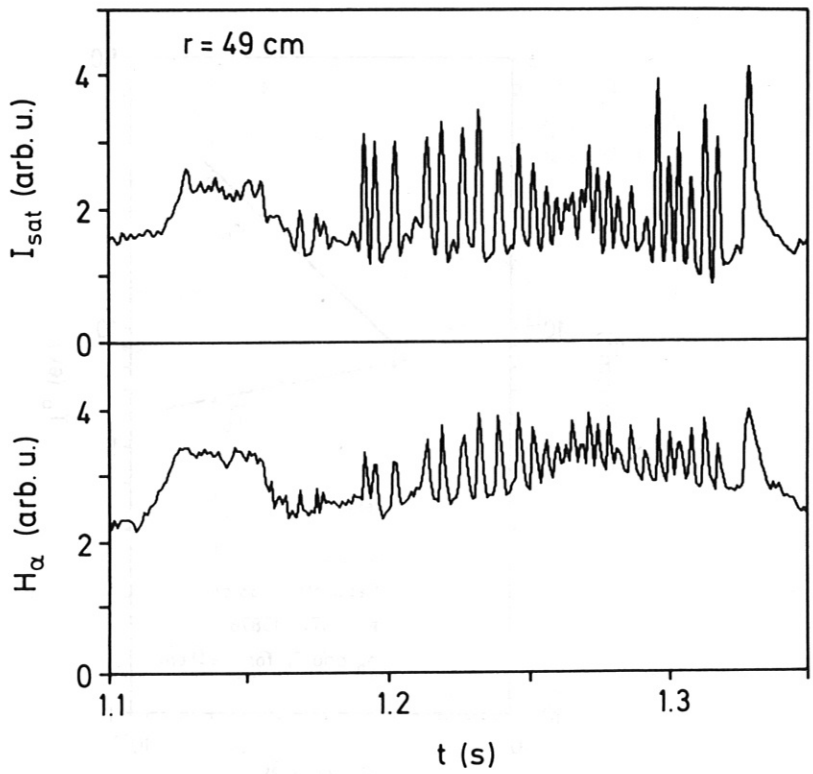

Fig. 9:
Comparison between the probe ion saturation current and the signal given by a photodiode measuring in the divertor chamber during NBI.

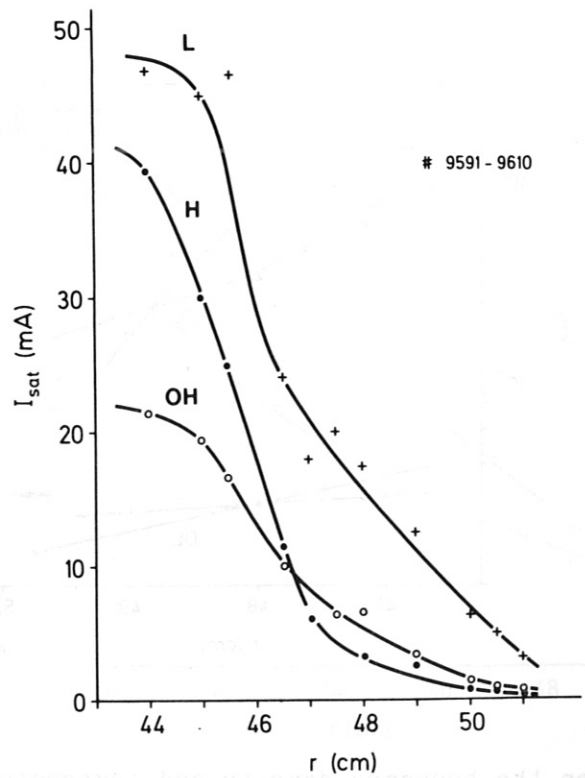

Fig. 10:
Probe ion saturation current radial profiles for the OH, L and H regimes.

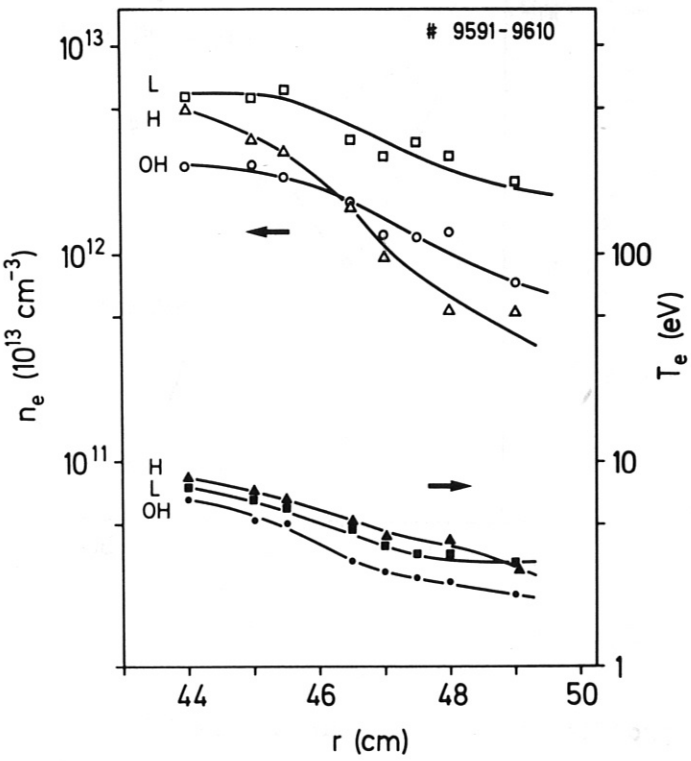

Fig. 11:
Radial profiles of denstiy and electron temperature for the OH, L and H regimes.

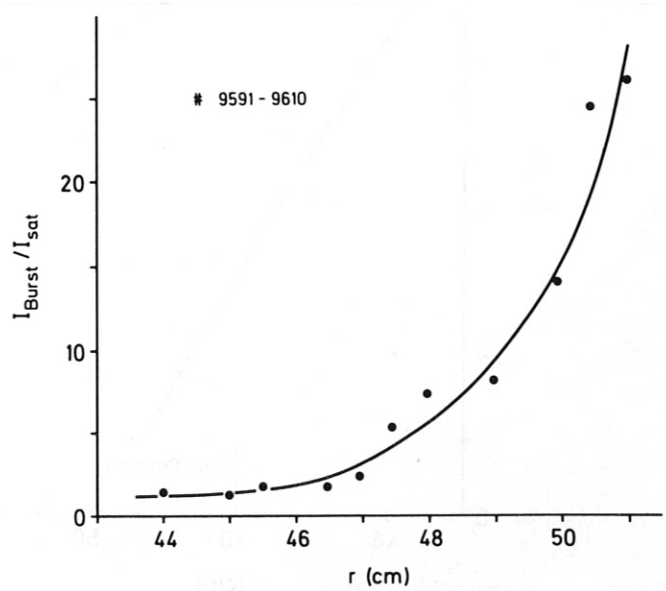

Fig. 12:
Relative increase in the burst current amplitude: I_{Burst} compared with the increase in the ion saturation current I_{sat} during the H regime.

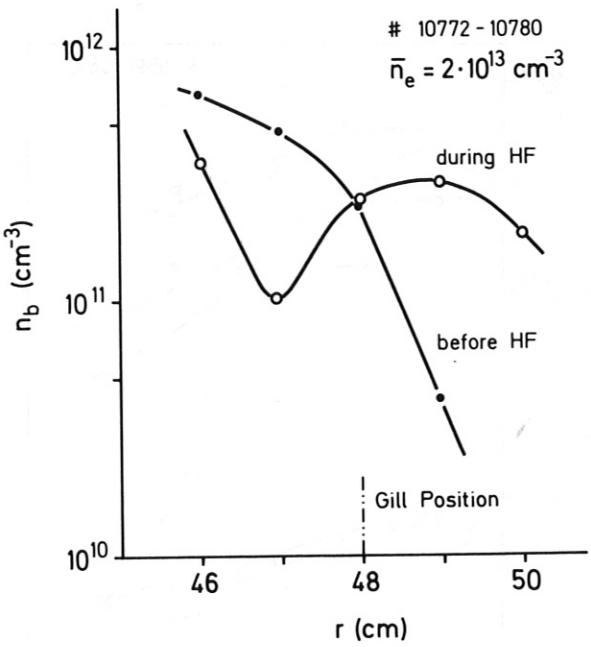

Fig. 13:
Radial density profiles before and during the HF.

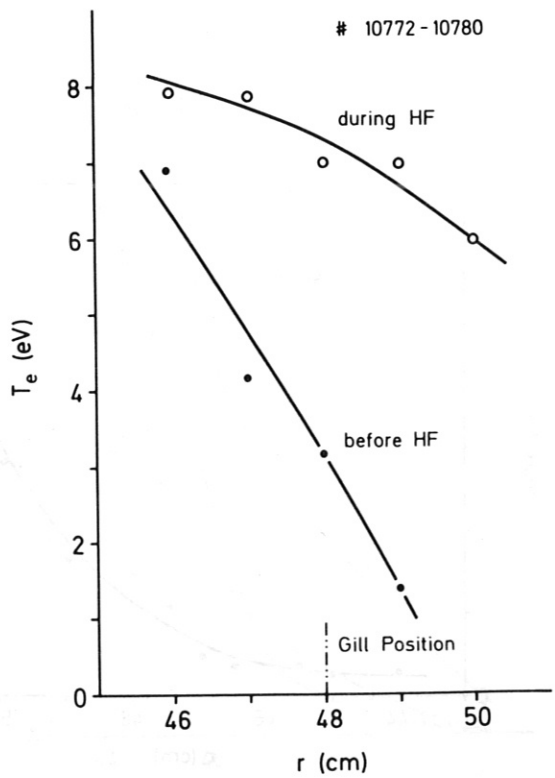

Fig. 14:
Radial electron temperature profiles before and during the HF.